

FREQUENCY FILTERING AND CONNECTED COMPONENTS CHARACTERIZATION FOR ZEBRA-CROSSING AND HATCHED MARKINGS DETECTION

Gavrilovic Thomas, Ninot Jérôme and Smadja Laurent

VIAMETRIS, Maison de la Technopole, 6 rue Leonard de Vinci, BP0119, 53001 Laval cedex, France, www.viametris.fr

Commission III, WG III/3

KEY WORDS: image processing, road marking extraction, frequency analysis, special marking recognition, Inverse Perspective Mapping

ABSTRACT:

In this paper, a new method for the detection and recognition of “repeating” markings such as hatched area, zebra-crossing, chevrons and “give way” markings is proposed. The detection of these kinds of markings is a manifold challenge. Besides being able to localize them (useful, *e.g.*, for markings database constitution or for Advanced Driver Assistance Systems), their detection may help to improve the efficiency of other algorithms like the detection and the recognition of continuous and dashed lines.

This article describes our three-step algorithm. First step is to segment markings on image. This process is a difficult task due to shadows on the road and because of deterioration and dirtiness of markings. Several line extraction techniques are compared in order to determine which of them can be considered to best filter noise on road image. This result is extended to extract larger markings (hatched markings, zebra-crossing, arrows). Then the following of the treatment is to filter candidate markings in the frequency and spatial domains according to their characteristics. Results of this algorithm are validated on a significant image set.

1 INTRODUCTION

Many applications use road markings detection and recognition through image processing. First of them is Advanced Driver Assistance Systems (ADAS) (*e.g.* lane departure warning system uses to alert driver of unintentional crossing lines). More and more cars will be equipped with these systems in the coming years. Another application is the road survey used to map a road by the passage of a vehicle equipped with a geolocation system. This allows a fast identification of the characteristics of a road network (road markings, traffic signs, curvature of the road...) in order to provide additional information : sight distance for road safety, road signs relevance, road marking quality. Other applications still exist as a pedestrian crossing detection system for the Partially Sighted.

Some research has been conducted to detect, track and recognize continuous and dashed lines. Others have allowed the recognition of zebra-crossing or arrows. Nevertheless, to our knowledge, there is still no specific algorithm for detecting hatched areas. Current zebra-crossing detection mainly use edge detection and classification. This method is employed on stereo images (Soheilian et al., 2006), for a single camera system with the calculation of cross ratio on edge (Muroi et al., 2008) or combined with a vanishing point detection for Partially Sighted vision (Se, 2000). There is also a method using projective invariant (Uddin and Shioyama, 2005). However, these techniques apply specifically on the detection of zebra-crossings and should not apply on hatched areas which differ from their dimensions, orientation and the relative position of their lines. It should also be noticed that the length of hatching lines are not uniform unlike zebra-crossing.

There are many aims that led to the development of this algorithm. In addition to being able to detect hatched area, this detection can also improve results of other marking recognition algorithms. In particular, our line marking detection algorithm, presented in part 3, can partially fail when there are too much markings around the processed pixel (see pictures a and b of figure 11). The reason is that algorithm uses a local threshold depending on the value of neighboring pixels. The removal of such image area

may be a good alternative to solve this problem. This algorithm can be used on a driver assistance system too. It can detect if a vehicle is driving on a way with hatching lines whereas it is prohibited. The presented algorithm is not limited to identify hatched area. Its process can also detect zebra-crossing and “give way” markings. The algorithm must be as robust as possible to cope with the different types of road traffic (city, country or highway).

In the next part, we will focus on preliminary work which consists on the elimination of perspective effect. Then we will describe our three-steps method. First, several road markings extraction algorithms will be compared to find which of them presents the best results. The two other steps consist in filtering candidate markings. Frequency and spatial filtering based on the characteristics of searched marking are used. The document outlines the approach to adopt for extracting hatched area, but a generalization of the result for zebra-crossing and “give way” marking is introduced into the last part of the document. Results of the algorithm are studied to determine its effectiveness on a significant image set.

2 INVERSE PERSPECTIVE MAPPING

We developed an acquisition vehicle for road surveying equipped with a high definition front side camera and a precise positioning system. Controller Area Network (CAN-bus) is used in order to acquire an image every 5 meters. We use gray scale images because the treatment on color images is slower and not significantly better (Veit et al., 2008). The first step of the treatment is to remove the perspective effect of the acquired image. This leads to obtain a bird’s eye view of the road which often simplifies marking detection and speeds up the process. In fact, perspective on image involve the use of variable dimension neighborhood according to the place of the processed pixel on the image. Inverse Perspective Mapping (IPM) (Bertozzi et al., 1998) is often used to obtain a resampled image (Rebut et al., 2004) (Sehstedt et al., 2007). Let us consider :

- $\mathbf{I} = (u, v) \in \mathbf{E}^2$ represents the 2D image space

- $\mathbf{W} = (x, y, z) \in \mathbf{E}^3$ represents the real 3D world space

\mathbf{I} is the space of the acquired image. The xy plane of the remapped image is the surface \mathbf{S} such as $\mathbf{S} = \{(x, y, 0) \in \mathbf{W}\}$ assuming the flatness of the road. We consider that this hypothesis is respected because the computation considers a short range; remapping is applied on the 30-meters area in front of the vehicle. To use the IPM transform, the knowledge of the following parameters is needed (see figure 1) :

- the position of the camera $\mathbf{C} = (l, d, h) \in \mathbf{W}$
- the direction of its optical axis : its yaw γ and its inclination θ ,
- its horizontal and vertical angular aperture : 2α and 2β
- its resolution : $m \times n$

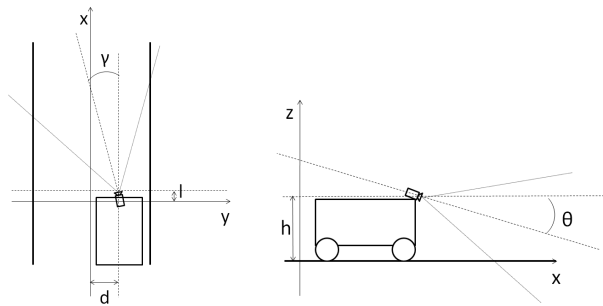


Figure 1: Parameters used in Inverse Perspective Mapping (Bertozzi et al., 1998)

For each pixel $(u, v) \in \mathbf{I}$, the following equation returns its position $M(x, y, z) \in \mathbf{S}$:

$$M = \begin{pmatrix} h \cdot \cot\left[\gamma - \alpha + u \frac{2\alpha}{m-1}\right] \cdot \cos\left[\theta - \beta + v \frac{2\beta}{n-1}\right] + l \\ h \cdot \cot\left[\gamma - \alpha + u \frac{2\alpha}{m-1}\right] \cdot \sin\left[\theta - \beta + v \frac{2\beta}{n-1}\right] + d \\ 0 \end{pmatrix} \quad (1)$$

Image resulting of this transformation are shown on figure 2.



Figure 2: Original and remapped images

3 ROAD MARKING EXTRACTION

3.1 Road lane detection

The first step of the algorithm presented in this article is to extract markings from the one channel remapped image. The main difficulty to extract road marking from an image is the difference of illumination on road due to shadows. A pixel representing road could have a greater intensity than a shadowed marking pixel. Fortunately, most of road marking are oriented along the road

(lines, dashed lines, zebra-crossing, arrows, hatched markings). On each line of the image, a marking appears as an horizontal white segment, considering that the vehicle is almost parallel to the road. This leads us to process the image line by line with a neighborhood of adequate width. This present section introduces our work for the road lane marking detection. With the aim of comparing different extraction approaches, a reference database named ROMA¹ including manually labeled ground truth images, was proposed (Veit et al., 2008). We use the same image database to develop and compare our algorithms. Three of implemented filters are presented : morphological opening, mean and median filter. For each of them, several neighborhood dimensions were tested in order to know the best to apply. It is important to notice that the line maximum width markings is 30 centimeters in the image database. The evaluation of the algorithm performance was made through Receiver Operating Characteristic (ROC) and Dice Similarity Coefficient (DSC, also named F-measure) curves. Usually, we consider an algorithm is better than another when its ROC curve is clearly above the others. However, when the curves cross, this measure is ambiguous and we thus take the DSC curve and its maximum value into account.

3.1.1 Mean filter The mean filter consists in adapting a threshold according to the local mean of the image intensity. Let (x, y) be the current pixel position, and $I(x, y)$ its intensity. We define mean operation applied to the pixel (x, y) of an image $I(x, y)$ using a neighborhood K of size B as:

$$\bar{I}_B(x, y) = \text{mean}_{z \in K} \{I(x, z)\} \quad (2)$$

The mean filter consists in testing if $I(x, y) - \bar{I}_B(x, y) > T_G$ with T_G a global threshold to apply on image. By experimentation (figure 3), we find that the best size for neighborhood width is 0.60 meter but it is difficult to find a correct explanation to justify it.

3.1.2 Opening filter Unlike mean filter, the morphological opening preserves strong edges of the image. It consists in calculating a morphological erosion followed by morphological dilation. As we are working with horizontal neighborhood, this processing removes all the luminance peaks with a width smaller or equal to the size of the structuring element.

We define the morphological opening operation applied to the pixel (x, y) as:

$$O_B(I)(x, y) = \delta_B(\epsilon_B(I)(x, y)) \quad (3)$$

where both erosion and dilatation operations are defined as:

$$\begin{cases} \epsilon_B(I)(x, y) = \inf_{z \in K} \{I(x, z)\} \\ \delta_B(I)(x, y) = \sup_{z \in K} \{I(x, z)\} \end{cases} \quad (4)$$

The opening filter consists in testing $I(x, y) - O_B(I)(x, y) > T_G$ for each (x, y) . $O_B(I)$ is able to remove pixels of road markings as soon as there is one pixel of road in the structuring element. So, markings clearly appear on the image resulting of $I - O_B(I)$. The size of the structuring element must be at least as large as the size of the searched marking. But, the wider the structuring element is, the less filtered the noise is. We deduce that the neighborhood should be the number of pixels equivalent to 30 centimeters plus one pixel to be certain to take one road pixel. Experimental results confirm our computation as can be observed in figure 4.

¹available at <http://www.lcpc.fr/en/produits/ride/>

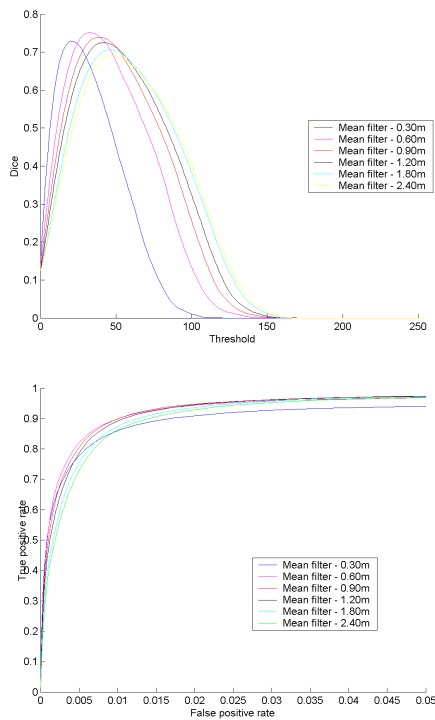


Figure 3: DSC and ROC curves of mean filter with different sizes of neighbourhoods.

3.1.3 Median filter The median filter is another smoothing filter and like morphological opening, also preserves strong edges. The median operation M is define as :

$$M_B(I)(x, y) = \text{median}_{z \in K} \{I(x, z)\} \quad (5)$$

The median filter consists in testing for each (x,y) if $I(x, y) - M_B(I)(x, y) > T_G$. The median function can be described as the number separating the upper half of a sample from the lower half. Thus, we deduce that the size of the neighborhood should be at least twice the number of pixels corresponding to 30cm (*i.e.* 60cm) plus one pixel to be certain to separate two populations with equal numbers of pixels. Then the median value will correspond to the supplementary pixel which belongs necessarily to the road. Figure 5 confirms this assumption.

3.1.4 Filters comparison We can evaluate the best result of each algorithm. Studying figure 6, we conclude that the best filter is that based on the median. Moreover, we use (Perreault and Hébert, 2007) to have a fast computation time.

3.2 Extension to special marking

According to (Veit et al., 2008) results and ours, median filter seems to be the best way to extract line marking. By extension, we believe that we will reach to the same conclusion for larger road markings (zebra crossing, hatched markings, arrows). Unfortunately, this study has not been achieved yet because of a lack of data. In order to detect hatching lines and according to the specifications of this kind of marking (line width of a hatched marking is about 0.75 meter, see discussion in the next chapter), the neighborhood size must be at least $2 \times 0.75 = 1.50m$ for median filter. In practice, we will take a 2.5 meters neighborhood to take surrounding line markings into account. Segmented image includes both the special markings and lines because their width are smaller than half the neighborhood size. Line markings can't

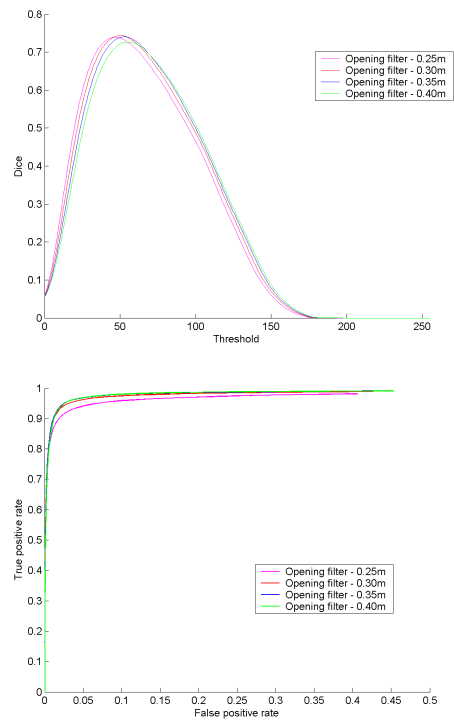


Figure 4: DSC and ROC curves of morphological opening filter with different sizes of neighborhoods.

be filtered depending on their width in order to preserve hatched markings extremities. So a way to identify extracted markings must be found.

Images of different stages are displayed on figure 7. Median images are computed and subtracted to original image. The value of the global threshold applied on resulting image is the one which presents the best result on DSC curve (34).

4 FREQUENCY FILTERING

4.1 Hatched markings specifications

In France, hatched markings are painted on roads depending on strict specifications. A hatching line is a white parallelogram. Its width is 50 centimeters but its length may vary from 50 centimeters to several meters. The slope of hatching lines (angle between long and short sides) must be 50 percents. There is an interval of 1.35 meter between each of them. So, the hatched area is a repeating pattern along the road which is surrounded by continuous line.

4.2 Discrete Fourier transform

The Discrete Fourier transform (DFT) is the sampled Fourier Transform. It does not contain all frequencies forming an image, but only a set of samples which is large enough to fully describe the image spatial domain. The number of frequencies corresponds to the number of pixels in the spatial domain image, *i.e.* the image in the spatial and Fourier domain have the same size. The results of DFT is composed by complex numbers which can be displayed with two images, either with the real and imaginary part or with magnitude and phase. In this paper, only the magnitude of the DFT is used as it contains most of the information of the image geometric structure on spatial domain. However, in order to transform the Fourier image back into spatial domain after

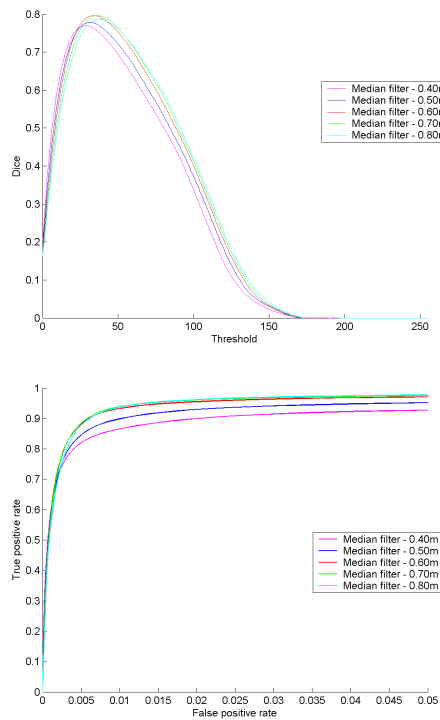


Figure 5: DSC and ROC curves of median filter with different sizes of neighborhoods.

some filtering in the frequency domain, we must use both magnitude and phase of the Fourier image. The 2D Discrete Fourier Transform (DFT) is defines as:

$$F(u, v) = \frac{1}{\sqrt{MN}} \sum_{x=0}^{M-1} \sum_{y=0}^{N-1} f(x, y) \exp^{-j2\pi(ux/M+vy/N)} \quad (6)$$

where $f(x, y)$ is a digital image of size $M \times N$.

The 2D Inverse DFT is defines as:

$$f(x, y) = \frac{1}{\sqrt{MN}} \sum_{u=0}^{M-1} \sum_{v=0}^{N-1} F(u, v) \exp^{j2\pi(ux/M+vy/N)} \quad (7)$$

4.3 Application for hatched markings detection

DFT is applied on binary image (Figure 7-d) in order to characterize hatched markings in frequency domain. The result is shown on figure 8-B.

In the following of the document, we will name right (resp. left) hatched markings, the hatched area composed of diagonal hatching lines going to the right (resp. left). On figure 2, we can see right hatched markings on the left of the image and left hatched markings on the right.

According to the hatched markings specifications seen in 4.1, there should be a principal frequency axis on DFT image when a hatched area is present on the image. The orientation of this axis is known and depends on the type of hatched markings. Moreover, there will be frequencies corresponding to other road markings extracted in part 3. However, these markings orientation (lines, zebra-crossing) is along the axis of the road. So, their frequency representations are along the horizontal axis of the frequency image.

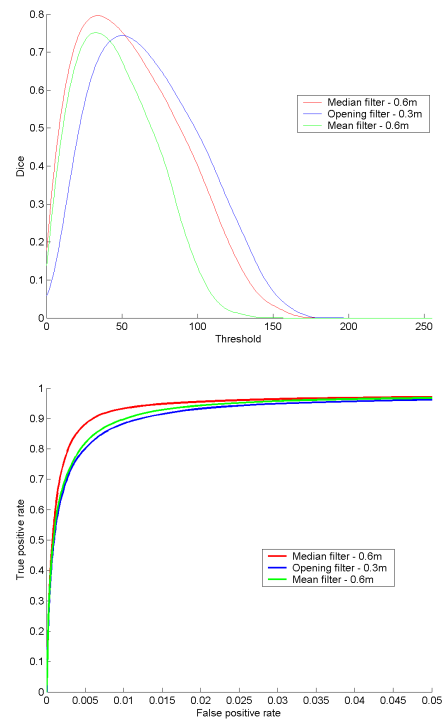


Figure 6: DSC and ROC curves comparing previous algorithm

To keep only frequencies of interest, it is possible to apply a mask in the frequency domain. In order to keep Right and Left hatched markings, two kinds of masks have been created, retaining central pixel (mean intensity of the image) and the axis of hatched markings frequencies with a margin (figures 8-C and 8-D). We obtain two frequency images (8-E and 8-F), used to go back on spatial domain. Frequency filtering tends to accentuate the pixels along the frequency retained after returning in the spatial domain. Therefore it may be useful to compare the result with the original binary image. A pixel that was not initially marking should not be retained. Images 8-G and 8-H result from this operation.

5 CONNECTED COMPONENTS CHARACTERIZATION

In this part, the goal is to detect special markings on filtered images. Connected component analysis is used to analyze regions in binary images. Connected component labeling is an algorithmic application of graph theory, where subsets of connected components are uniquely labeled. This approach allows to characterize each connected component (dimensions, main axis direction, eccentricity) in order to find subsets which respect marking properties.

5.1 Principal axis extraction

An important characteristic of a connected component is its principal axis. It allows to extract long and short sides length of connected pixels. In order to extract main axis, we firstly use image moments. Image moments are useful to describe objects after segmentation. Image properties such as image centroid or orientation can be easily computed. Nevertheless, the orientation found by this method tends to be the diagonal of extracted road marking. Another solution is to use the least squares technique. For each marking, we apply it on centers of their vertical segment. The result can be shown on figure 9.

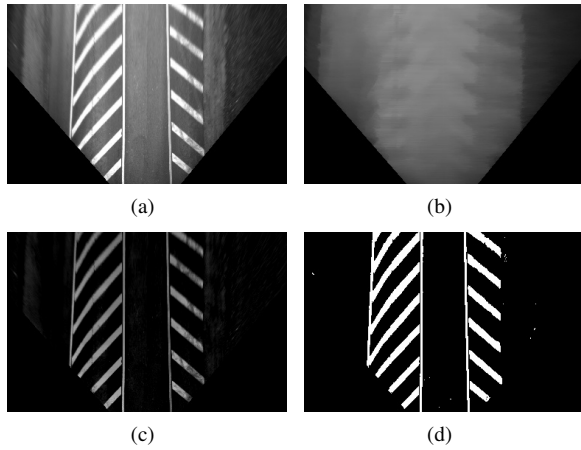


Figure 7: Median filter segmentation result with a 1.2m neighborhood sized. (a) Original image, (b) Median image, (c) Subtraction of median image, (d) Thresholding

5.2 Dimension filtering

After finding the orientation of each marking, those did not match to spatial expected characteristics are filtered out. To do that, the median width and length of connected components are calculated compared to the main axis. A 10% margin is taken from the marking specification. For example, a candidate marking must be 50 ± 5 centimeters wide to not be filtered for hatched marking detection.

5.3 RANSAC

Final step of the treatment consist in use RanSaC algorithm((Fischler and Bolles, 1981)) with marking candidate. On the road, every line marking belonging to the same set (hatched area, zebra-crossing) have the same orientation. So, we apply RanSaC on connected component that have the same orientation (± 5 degree). A connected component is an inlier if RanSaC line model is passing through it. Line model is considered to be exact if it has more than three inliers. To arrange detected hatched area, it is possible to calculate the convex hull which envelop the extremity of every inliers markings. IPM can be used to display hatched area in the original image. The result is shown on figure 10.

6 RESULTS AND DISCUSSION

6.1 Application on road lane detection

The detection of hatched areas allows us to improve our road lane detection. In fact, hatched area tends to harm this detection. We find in part 2 that the best filter to apply on image is median filter. But with a neighborhood adapted to the detection of road lines (about 30 centimeters), the median filter will not detect marking near hatched areas because median value of neighborhood will be a road marking value. So, there will have some gaps in continuous line because segment is not enough large to be consider as a line marking(see figures 11-a and 11-b). Marking recognition will find dashed lines instead of continuous line on the road. A solution to avoid that is to replace every pixel in the detected hatched area with the value of pixel resulting from median filter with a neighborhood adapted to hatched marking. The neighborhood of each marking line will be composed of road pixel so the detection and recognition will be correct (figure 11-b and 11-d).

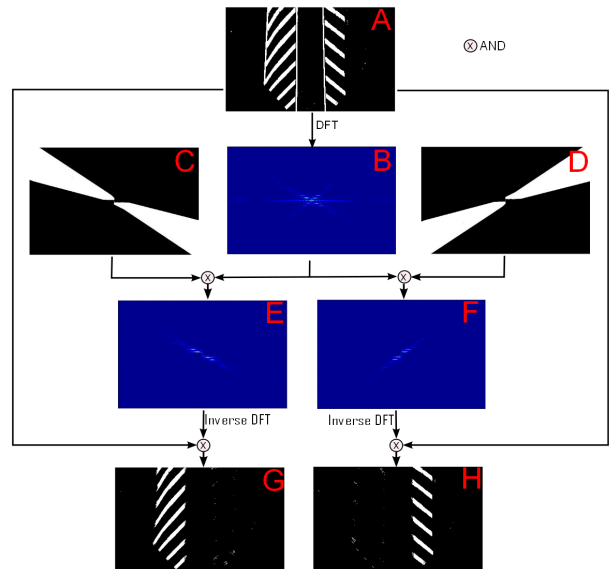


Figure 8: Different steps of frequency analysis : A) Initial image, B) DFT transform, C)-D) Frequency masks, E) - F) DFT after masking, G)-H) Final images

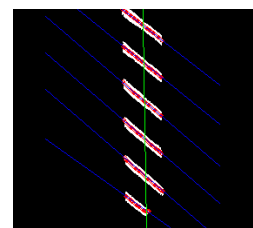


Figure 9: RanSac algorithm applied on left hatched markings. Red points correspond to the middle of column segment. Blue lines are the principal axis of each connected component. Green line is the result of RanSac algorithm.

6.2 Extension for other markings

This algorithm can be also used to detect chevron marking. Indeed, chevrons are composed of two surfaces : a left and a right hatched areas. So, the addition of this two areas gives a chevron. The advantage of the algorithm is also the possibility to detect other types of marking with minimal changes. To detect zebra-crossing and “give way” markings, one just has to change the size of the neighborhood in marking extraction step. These markings are 0.50 meter wide, so we consider a $2 \times 0.50 = 1\text{m}$ median filter. We use a specific frequency mask filtering non-horizontal frequencies. Connected component characteristics need also to be modified : a 50 centimeters width is used for zebra-crossing detection plus a length of 50 centimeters for “Give Way” detection.

6.3 Evaluation on image set

In order to evaluate our detection algorithm for hatched area and zebra-crossing, we apply it on an image set grabbed with our vehicle. Used camera has a resolution of 1920x1080. Images were acquired in normal circulation conditions on a 50 km long circuit with various road conditions (primary and secondary road network). The image database is composed of 9866 images including 93 images of zebra-crossing and 30 hatched areas visible



Figure 10: Extracted hatched area in blue

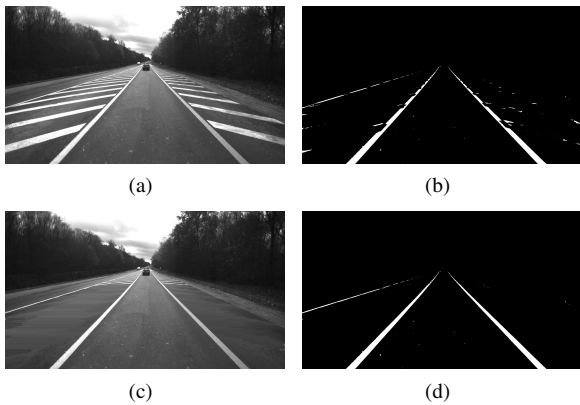


Figure 11: (a)-(b):Original image and road marking extraction, (c)-(d):After removing hatched area and its road line extraction

on 308 images. Table 1 summarizes our result. Hatched marking and zebra-crossing detection failed on some images because of the extraction on damaged markings or because of too small hatched areas. False positives are mainly due to reflections on some vehicles.



Figure 12: Example of experimental images with algorithm result. Blue areas represent hatching lines detection and green one represent zebra-crossing detection.

7 CONCLUSION AND FUTURE WORK

In this paper, a new technique for the detection of “repeating” marking on images grabbed with a front side camera has been introduced. Some of our road marking detection methods have been compared to existing works and we concluded that median filter seems to be the best option. In the following stage, the characterization of connected components in frequency and spatial domains allows to extract markings of interest according to their characteristics. More generally, this technique can be used to find repeating road marking patterns on a bird’s eye view. Very

	Correct marking detection	Number of false positive
Hatched marking	301 / 308 (98%)	5
Zebra-crossing	88 / 92 (96%)	3

Table 1: Results of hatched marking and zebra-crossing detection on a 9866-images set

promising results have been obtained from this algorithm, which can be easily implemented and presents a quite fast execution time (about 70 km per hour with a 2GHz processor). Moreover, it improves road lane detection when used as a preprocessing step, preventing road line extraction from misdetection.

Next stage of development will consist in taking into account the vehicle position with respect to the road (e.g. by using a road segmentation algorithm) to precisely adjust our models to specific cases (occurring when the vehicle is turning).

REFERENCES

- Bertozzi, M., Broggi, A. and Fascioli, A., 1998. Stereo inverse perspective mapping: Theory and applications. *Image and Vision Computing* 16(8), pp. 585–590.
- Fischler, M. A. and Bolles, R. C., 1981. Random sample consensus: a paradigm for model fitting with applications to image analysis and automated cartography. *Commun. ACM* 24(6), pp. 381–395.
- Muroi, H., Shimizu, I., Raksincharoensak, P. and Nagai, M., 2008. Pedestrian recognition by a single camera for driver assistance. In: *Proceedings of FISITA 2008 World Congress*, Munich, Germany, pp. F2008–08–118.
- Perreault, S. and Hébert, P., 2007. Median filtering in constant time. *IEEE Transactions on Image Processing* 16(9), pp. 2389 – 2394.
- Rebut, J., Bensrhair, A. and Toulminet, G., 2004. Image segmentation and pattern recognition for road marking analysis. In: *IEEE International Symposium on Industrial Electronics*, Vol. 1, Ajaccio, France, pp. 727 – 732.
- Se, S., 2000. Zebra-crossing detection for the partially sighted. In: *Proceedings of the IEEE Computer Society Conference on Computer Vision and Pattern Recognition (CVPR’00)*, Vol. 2, Hilton Head, SC, USA, pp. 211 – 217.
- Sehestedt, S., Kodagoda, S., Alempijevic, A. and Dissanayake, G., 2007. Robust lane detection in urban environments. In: *Proceedings of IEEE/RSJ International Conference on Intelligent Robots and Systems (IROS)*, San Diego, CA, USA, pp. 123–128.
- Soheilian, B., Paparoditis, N., Boldo, D. and Rudant, J., 2006. 3d zebra-crossing reconstruction from stereo rig images of a ground-based mobile mapping system. *International Archives of Photogrammetry, Remote Sensing and Spatial Information Sciences* 36 (Part 5), pp. (on CD-ROM).
- Uddin, M. S. and Shioyama, T., 2005. Bipolarity and projective invariant-based zebra-crossing detection for the visually impaired. In: *Proceedings of the IEEE Computer Society Conference on Computer Vision and Pattern Recognition (CVPR’05)*, Washington, DC, USA, p. 22.
- Veit, T., Tarel, J.-P., Nicolle, P. and Charbonnier, P., 2008. Evaluation of road marking feature extraction. In: *Proceedings of 11th IEEE Conference on Intelligent Transportation Systems (ITSC’08)*, Beijing, China, pp. 174–181. <http://perso.lcpc.fr/tarel.jean-philippe/publis/itsc08.html>.